POLITECNICO
MILANO 1863

SCUOLA DI INGEGNERIA INDUSTRIALE
E DELL'INFORMAZIONE

Executive Summary of the Thesis

Clustering Neuron Population Spike Data and Assessing Cortical Area Connectivity

Laurea Magistrale in Biomedical Engineering - Ingegneria Biomedica

Author: Reza Asri

Advisor: Prof. Alessandra Pedrocchi

Co-advisor: Dr. Sylvain Crochet

Academic year: 2022-2023

The dissertation was conducted at the Laboratory of Sensory Processing at EPFL

1. Introduction

The interpretation of incoming sensory information from the outside world to guide adaptive behavior is a crucial function of the brain. A fundamental question in neuroscience is how and where sensory information is translated into motor commands in a context- and learning-dependent manner. Studies have demonstrated a gradual transformation of sensory signals into decision/motor signals from sensory to frontal areas: primary sensory areas encode primarily the physical features of the stimulus, whereas the response of frontal areas (such as the prefrontal cortex) covaried with both the decision and the physical features of the stimulus. Thus, it has been argued that flexible sensorimotor decisions result from the integration of sensory and task information in the prefrontal cortex. The medial prefrontal cortex (mPFC) is assumed to play a fundamental role in context-dependent behaviors.

To determine which neurons are involved in a particular aspect of sensorimotor task, an unsupervised clustering algorithm developed to explore the neural behavior of a large recorded population of neurons and their hypothesized roles more precisely. By defining the properties of neurons within a specific group, the researcher can then determine functional classes of neurons depending on their relationship to the task. Gaussian mixture model (GMM) is among the most used algorithms for the clustering the neurons of the sensorimotor areas [3]. The concept is based on collecting significant features from the firing rate and clustering them using an expectation-maximization Gaussian mixture algorithm (EM-GMM) [5]. The approach can automatically detect and cluster similar firing rate profiles based on specific signal characteristics.

In a different study, to investigate the role of learning in the modification of synaptic connections and assess brain plasticity, functional connectivity study of neuron-to-neuron or network-to-network was utilised. Neural plasticity, also referred to as neuroplasticity or brain plasticity, is the capacity of the nervous system to change its activity in response to intrinsic or extrinsic stimuli by reorganizing its structure, functions, or connections. Through the synaptic connections, brain cells construct the neural circuits that support our sensory, motor, and cognitive abilities and eventually govern our entire behav-

ior. The correlation which exists between the firing activity of cortical neurons, are thought to be a key in processing of many neural systems; hence, the functional connectivity by correlation analysis was evaluated. Correlated neurons fire at similar times but not precisely synchronously; therefore, correlation must be described in terms of a timescale within which spikes are considered correlated. Also, spiking is sparse regarding the recording's sampling frequency and spike duration. This implies that conventional approaches to correlation (such as Pearson's correlation coefficient) are inappropriate, as periods of quiescence should not be counted as correlated and correlations should compare spike trains over short time frames, not just instantaneously. So, to be more precise and to overcome the flaws of correlation analysis in spike data, researchers used spike time tiling coefficient (STTC) method [2]. The spike time tiling coefficient uses the proportion of the recording that falls within delta t of spikes from neuron A to evaluate if the proportion of spikes in neuron B that share this property is indicative of the correlation. Cross-correlogram method was also implemented to assess mono-synaptic directional connectivity [6] as neurons in the cerebral cortex create thousands of synapses with other cortical neurons in nearby and distant brain regions and have descending and recurrent connections with subcortical systems.

2. Methods

Data used in clustering and connectivity projects are respectively titled as "Psychometric detection task" and "Delayed response detection task" gathered by neuroscientists at EPFL's laboratory of sensory processing.

2.1. Psychometric detection task

Mice were trained head-restrained to perform a whisker dependent tactile detection task during which a brief passive C2 whisker stimulation is present and mice respond by licking a spout in order to obtain a reward (Figure 1A). The whisker stimulation was achieved by attaching an iron particle to the C2 whisker (1 mm from the pad) at the beginning of each training session. A magnetic coil placed directly below the mouse's head produced a 1 ms magnetic pulse, which was subsequently used to induce a small and rapid whisker movement. Over sessions, mice learned to lick in response to the whisker stimulus within the one second response window after stimulus onset. Mice were also required not to lick for a variable 2.5-3.5 s 'No Lick' window in order to initiate a new trial (Figure 1B). Mice were presented with four different whisker stimulation amplitudes from very low (1 degree) to salient (3.3 degree) randomly interleaved during the behavioral session. Trials when the mouse licked the reward spout within the 1 second response window after whisker stimulation, were considered as "hit trials", and rewarded with the sweet water; if the animal did not lick within one second of response window after whisker stimulation no reward was delivered, and these trials were considered as "miss trials"; trials when no whisker stimulation were delivered (catch trials), but the mouse licked the reward spout were considered as "false alarm trials"; if no licking occurred during catch trials, they were considered as "correct rejection". Once the performance of the animal reached a stable and satisfactory level (more than 70 percent of hit rate and less than 30 percent of false alarm for the strongest amplitude), an acute extracellular recording session was performed using silicon probes as mice performed the psychophysical task. Two areas out of three areas were recorded simultaneously so, in each session, two probes were implanted into two distinct brain sites.

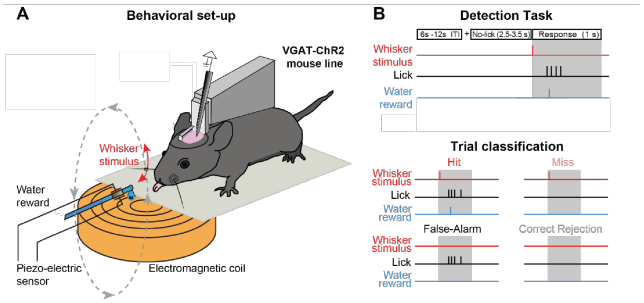

Figure 1: (A) The experimental setup for the whisker-based detection task. Mice were head-restrained in front of a water spout and above an electromagnetic coil.(B) Task structure. Animals were trained to respond to the whisker stimulation by licking the reward spout within the 1 s of the response window and to suppress licking for a random interval of 2.5-3.5s during no lick period.

2.2. Delayed response detection task

In another task, a go/no-go learning paradigm was designed where head-restrained mice learned to lick in response to a whisker stimulus after a 1-s delay period (Figure 2A- 2C). Each trial included a visual cue (200 milliseconds, green LED) and an auditory cue (200 ms, 10 kHz tone of 9 dB added on top of the continuous background white noise of 80 dB). The stimuli were separated by a delay interval that was gradually increased to 2 seconds during the course of the pretraining days. During the behavioral studies, all whiskers were trimmed with the exception of the C2 whiskers on both sides. Expert and Novice mouse groups underwent a pretraining phase consisting of trials with visual and auditory signals (without whisker stimulus) (Figure 2C). Mice were rewarded for licking a spout placed on their right side within one second after the onset of the auditory cue. Trials were separated by 6 to 8 seconds and began after a time of 2 to 3 seconds during which mice did not lick the spout. Licking before the response period (Early lick) aborted the trial and introduced a 3-5 s timeout. Mice learned to lick the spout by detecting the auditory cue and suppressing early licking after 3-6 days of pretraining. The electrophysiological recordings from the Novice group of mice was performed when mice finished the pretraining phase and were introduced to the whisker delay task (Figure 2C). In half of the trials, a whisker stimulus (10 ms cosine 100 Hz pulse through a glass tube attached to a piezoelectric actuator) was applied to the right C2 whisker 1 s following the beginning of the visual cue. Importantly, the reward was only accessible in trials with the whisker stimulus (Go trials), and mice who licked in trials without the whisker stimulus (No-Go trials) were punished with a time-out and an auditory buzz tone (Figure 2B). Thus, mice were trained to change their licking/non-licking behavior in response to the whisker stimuli. Since the whisker stimulus was weak, Novice mice continued to lick in the majority of Go and No-Go trials regardless of the whisker stimulus and exhibited no whisker learning (Figures 2D). The Expert mice entered a 2-29 day Whisker-training phase during which a stronger whisker stimulus (larger amplitude and/or pulse train) and shorter delays (for some mice) were introduced. As the mice learnt to lick properly, the whisker stimulus amplitude was gradually decreased and the latency was increased to 1 s, eventually achieving the same circumstances as novice mice. As measured by the piezoelectric lick sensor, expert mice decreased licking in No-Go trials but increased their premature early licks after the whisker stimulus (Figure 2D).

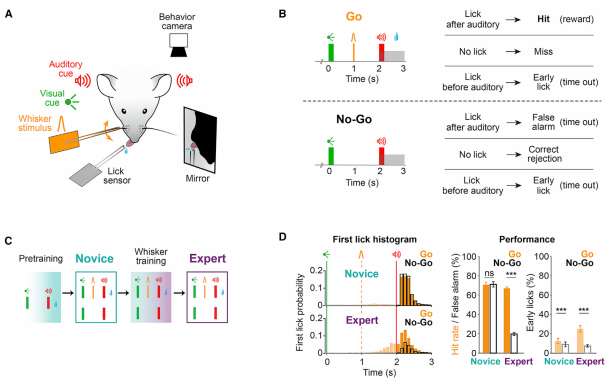

Figure 2: (A) Behavioral setup. Sensory stimuli were delivered to head-restrained mice. (B) Task structure and trial outcomes in go and no-go trials. (C) Learning paradigm. All mice went through visual-auditory pretraining, where all licks after the auditory cue were rewarded. Expert mice went through whisker training, where final task structure was used as in (B). (D) Task performance. Left: first-lick time histogram was similar in go versus no-go trials in novice mice but differed in expert mice. Early licks are shown with light colors. Middle: novice mice licked equally in go and no-go trials, whereas expert mice licked preferentially in go trials (quantified as mean ± SEM across all completed trials). Right: both groups of mice made more early licks in go compared to no-go trials. *** indicates $p < 0.001$ according to Wilcoxon signed-rank test.

2.3. Clustering analysis of spike data

5 kinds of trials are included in the analysis; hit trials aligned both to whisker stimulus onset and to jaw opening onset; miss trials aligned to whisker stimulus onset; spontaneous licks happening in inter-trial intervals and aligned to the lick signal from piezo sensor on water spout; spontaneous whisking trials that are aligned to the onset of whisking. For each neuron and trial

type, time-varying PSTHs (100 ms bin size) were generated during a 2.5-s window beginning 1 s before the alignment and ending 1.5 s afterward (25 bins for each kind of trial). PSTHs from various trial types were baseline subtracted, normalized to the range of values across all bins (of all five trial types), and then concatenated, yielding an activity matrix $X \in R^{1598*125}$ whose row I corresponds to the concatenated normalized firing rate of the neuron I across various trial types and columns correspond to time bins (Figure 3). A general overview of steps taken for clustering is shown in Figure 4. To decrease the existing redundancy between firing rate time bins and speed up the computation, principal component analysis (PCA) was applied to linearly projected firing rate vectors onto a low-dimensional space removing correlated features before clustering. PCA was performed on the centered version of X (i.e.,$x_i - \bar{x}_i$) and identified nine significant components.

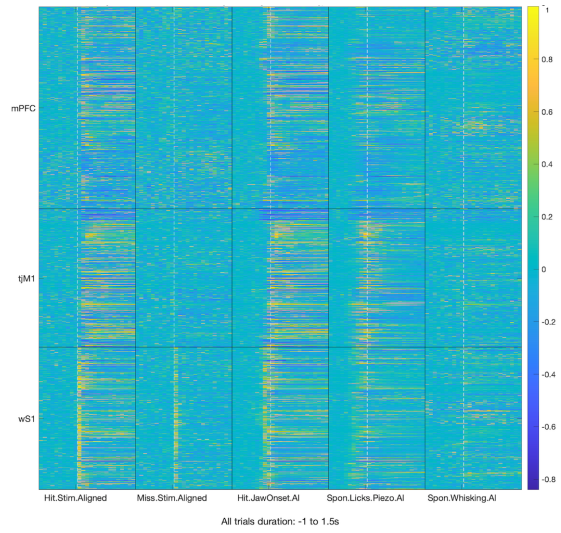

Figure 3: PSTH of matrix X. Color bar represents normalized firing rate.

By normalizing the data, the weight of distinct components was equalized, resulting in one variance for each component ($X' \in R^{1598*9}$). Next, spectral embedding was used to identify non-convex and more complicated clusters. To do this, the similarity matrix $S \in R^{1598*1598}$ was calculated, whose element at row I and column j measures the similarity between $x_i{}'$ and $x_j{}'$ as

$$s_{ij} = exp\frac{-||\, x_i{}' - x'\,||_2^2}{2\sigma^2} \in [0, 1],$$

where σ is a free parameter that determines how

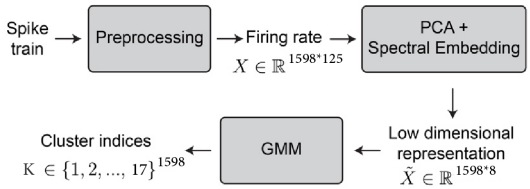

Figure 4: Block diagram indicating the different steps for unsupervised neuronal clustering. Dimensionality reduction and spectral embedding were applied on concatenated trialtype averaged PSTHs of neurons and the results were clustered by fitting a Gaussian mixture model (GMM).

local similarity is measured in the feature space. σ was calibrated by setting the average similarity value at 0.5. Then, the normalized Laplacian matrix was constructed using the formula

$$L = I - D^{-0.5} W D^{-0.5},$$

where I is the identity matrix and D is the diagonal degree matrix defined as $\mathrm{diag}(\{\sum_{k=1}^{1598} s_{ik}\}_{i=1}^{1598})$. The transformed features are rather abstract and computed as the eigenvectors of L. Notably, the new feature space is a non-linearly converted version of the PCA space, which itself is a linearly transformed version of the original firing rate space. Such a transformation is believed to naturally separate data points which are clustered together [1]. Using the elbow approach on the eigenvalues of matrix L (i.e., locating the sharp transition in the derivative of sorted eigenvalues), (after omitting the very first eigenvector) the first 8 eigenvectors of matrix L were considered as representative features, resulting in matrix $\tilde{X} \in R^{1598*8}$. Using a Gaussian Mixture Model (GMM), neurons were clustered based on the resulting matrix $\tilde{X}$. The approach assumes that the underlying data distribution is a combination of K Gaussians with means $\{\mu_1, ..., \mu_k\}$, diagonal covariance matrices $\{\sum_1, ..., \sum_k\}$, and weights $\{\rho_1, ..., \rho_k\}$. The parameters of this mixture model were computed using the expected maximization (EM) approach for a given K [3]. To do this, the 'fitgmdist' function in MATLAB (Mathworks) was utilized with 1,000 maximum iterations, 0 regularization value, 5000 replicates, and a diagonal covariance matrix constraint. This generates a GMM in which the principal axes of the Gaussians are parallel to the axes of the

feature space, providing greater flexibility than the k-means approach while preserving a limited number of fitting parameters. The number of clusters was then chosen (k = 17) by minimizing the Bayesian information criterion (BIC) (Figure 5). It is a penalized likelihood term defined as -2log(L) + Mlog(n), where log(L) is the data's negativelog-likelihood, M is the number of GMM parameters, and n is the number of observations. The first term rewards models with strong fit, whereas the second term penalizes models with greater complexity. Using the fitted parameters, each neuron was assigned a cluster index $k_i \in \{1, ..., 17\}$ corresponding to the Gaussian distribution to which it most likely belongs. The output of the GMM stage was the vector $K \in \{1, ..., 17\}^{1598}$ holding the neuron cluster indexes (Figure 7).

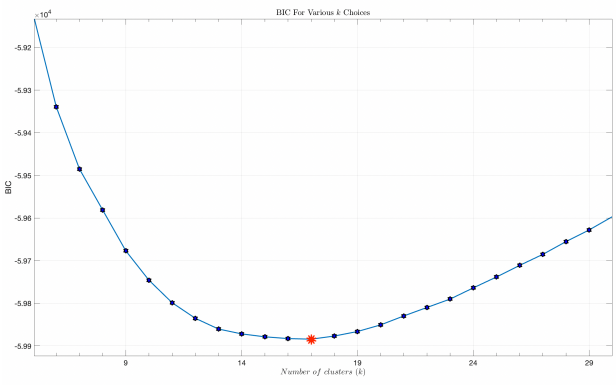

Figure 5: Determination of the number of clusters. Number of optimal clusters (k=17) was determined as the minimum of the Bayesian information criterion (BIC) curve.

To determine the amount that neurons from various brain regions contribute to each cluster composition, two steps were taken. First, the distribution of neurons within each cluster across distinct brain areas was assessed (Figure 9). Weighted proportions were evaluated to account for the disparities in the total number of neurons belonging to each group and brain area. To see how the neurons of a specific area are distributed across clusters, the same calculation of Figure 9 has been done with difference of normalization to the number of clusters instead of the number of areas (Figure 10). Finally, a "distribution index" (Figure 8) that measures the dispersion of each cluster across several brain areas was established. The total variation distance between the weighted distribution of neurons was calculated in each cluster across three brain regions and the uniform distribution for this purpose:

$$TV_k = \frac{1}{2} \sum_a \left| \rho_{k,a} - \frac{1}{3} \right|,$$

Where $\rho_{k,a}$ is the weighted proportion of cluster k neurons that belong to region a. Note that $\rho_{k,a}$ has been normalized with respect to areas, i.e., $\sum_a \rho_{k,a} = 1$. The distance TV_k has a minimum value of 0 when the neurons of cluster k are dispersed uniformly across all brain regions and a maximum value of $\frac{2}{3}$ when all neurons of cluster k belong to a single brain region. To scale this value between zero and one, a distribution index was constructed D_k for each cluster k as follows:

$$D_k = 1 - \frac{3}{2} TV_k \in [0, 1],$$

$D_k = 1$ implies that cluster k is uniformly distributed throughout brain regions, while $D_k = 0$ indicates that cluster k is concentrated in a single brain region.

2.4. Interareal connectivity analysis

Single units were isolated and separated into fast-spiking units (FSU) or regular spiking units (RSU) based on spike width. Utilizing the subset of sessions with simultaneous paired recordings from whisker sensory and motor cortices, the changes in the coordination of interareal wS(1,2)->wM(1,2) neural activity across learning were examined using two distinct techniques.

2.4.1 Pearson correlation

First, the Pearson correlation was determined between trial-by-trial whisker-evoked responses in pairs of individual neurons recorded from wS1/wS2 (5 to 55 ms after whisker onset) and wM1/wM2 (10 to 90 ms after whisker onset) (Figure 15). For the pair-wise correlation analysis, only neurons within the analysis windows whose average firing rate was greater than 2.5 Hz were examined. Similarly, the Pearson correlation between the trial-by-trial average population responses in the same task epochs between pairs of simultaneously recorded areas was calculated (Figure 17A).

2.4.2 Spike Time Tilling Coefficient

The STTC technique [2] was utilized as a second measure of pair-wise correlation, which is hypothesized to be insensitive to firing rate. The STTC was calculated during a 1-second window centered on the whisker stimulus (Figure 17B) and was defined for spike trains A and B as

$$STTC = \frac{1}{2}\left(\frac{P_A - T_B}{1 - P_A T_B} + \frac{P_B - T_A}{1 - P_B T_A}\right),$$

where P_A and P_B are the proportion of spikes from A falling within $\pm\Delta t(\pm 10$ ms) of a spike in B and vice versa and T_A and T_B are the proportion of the total recording time that falls within $\pm\Delta t$ of a spike from B or A, respectively (Figure 6).

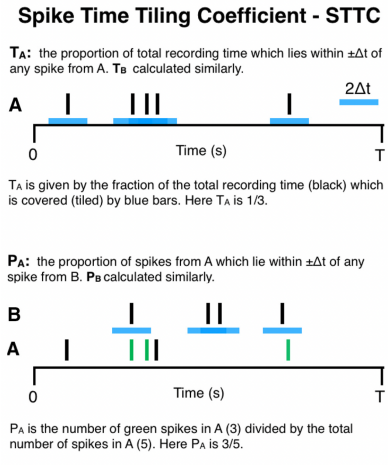

Figure 6: Diagram illustrating the spike time tiling coefficient computation. PA, PB, TA, and TB are the four parameters required to determine the spike time tiling coefficient. Δt is the only free parameter. Values and scales are only for illustrative purposes. Adapted from [2].

2.4.3 Cross-correlograms

In addition, directional functional connectivity from wS1 to wM1 and from wS2 to wM2 was determined using cross-correlograms (CCG) within a 1 second window centered on whisker stimulus (Figure 16, and 17).The CCG was defined as

$$CCG(\tau) = \frac{\frac{1}{M}\sum_{i=1}^{M}\sum_{t=1}^{N}\chi_1^i(t)\chi_2^i(t+\tau)}{\theta(\tau)\sqrt{\lambda_1\lambda_2}},$$

where M is the number of trials, N is the number of bins in the trial, χ_1^i and χ_2^i are the spike trains of the 2 units on trial i, τ is the time lag relative to reference spikes, and λ_1 and λ_2 are the mean firing rates of the reference and target units, respectively. $\theta(\tau)$ is the triangle function that corrects for the overlap of time bins resulting from the sliding window. Within the analysis window, neurons with a firing rate greater than 1 Hz were included in the analysis. Cross-correlograms were corrected by removing a jittered version [7] (Figure 17C) to better capture fast timescale changes related to feedforward connections

$$CCG_{corrected} = CCG - CCG_{jittered}$$

The jittered CCG was generated by averaging 100 resamplings of the original dataset in which spike times inside each 25-ms window were permuted randomly across trials. This technique eliminates stimulus-locked and slow timeframe correlations bigger than the jitter window while maintaining the trial-averaged PSTH and number of spikes each unit. The significant directional link from reference to target neuron was determined for each pair of recorded units if the maximum CCG within time lags between 0 and 10 ms was greater than the 6-fold standard deviation of the jitter-corrected CCG flanks (between ± 50 to 100 ms). For both analytical methods, in wS1/wS2, we concentrated only on RS units, which are known to have long-range projections. In wM1/wM2, correlations and directional connectivity were evaluated independently for RS and FS units.

3. Results

3.1. Clustering analysis of spike data

Unsupervised clustering of neurons was performed on the basis of their temporal firing pattern across several trial types (Hit, Miss, Spontaneous licks, and whisking) by combining neurons from different brain regions. Clustering based on the Gaussian mixture model (GMM) produced 17 groups of neurons (Figure 7), sorted by their onset latency. Next, a "distribution index" was calculated that measures the composition of clusters inside versus between areas (Figure 8). The low distribution index for wS1 clusters (1, 2, 3), tjM1 clusters (5, 8, 11), and mPFC clusters (6, 17) indicates their limited distribution in specific brain areas. In contrast, the dispersion

index was high for the other clusters, indicating that these clusters are widely distributed across brain regions.

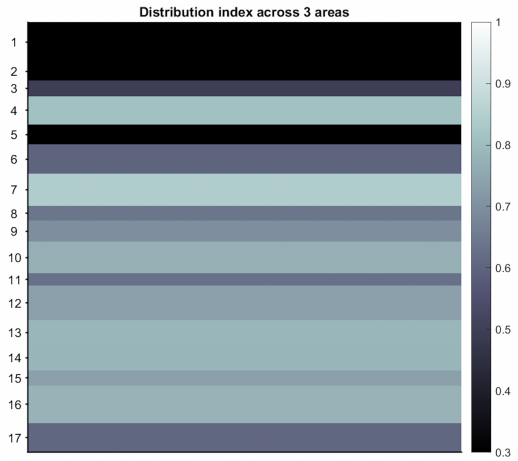

Figure 8: Distribution index between 0 (localized in one area) to 1 (uniformly distributed). Values are corrected for different sample size in different areas.

The neuronal clustering revealed some patterns of activity: (1) a rapid and transient increase in neuronal activity following the whisker stimulus (clusters 1–3), which was predominantly represented in wS1; (2) both inhibition (clusters 4) and excitation (cluster 5,7-11) mainly in tjM1; and (3) complex behaviours mainly in mPFC (cluster 6,12-17). cluster 1 and 2 are mostly composed by wS1 neurons, cluster 5 by tjM1 neurons, and cluster 6 by mPFC neurons indicating that there are specific patterns related to a specific area. Strikingly, the majority of clusters are represented by neurons of all three areas pointing to a distributed information codding and that similar neuronal responses can be found in all three areas.

3.1.1 How sensory information is represented by neuronal activity?

In figure 11, grand average PSTH of most representative clusters of wS1 is shown. We have sensory neurons in clusters 1, 2, and 3 with the major contribution of wS1 however, it is evident that mPFC is the second contributor in the composition of clusters 2 and 3 indicating the existence of sensory neurons in mPFC. Considering hit trials, there is a secondary lasting excitation in cluster 2 and a secondary lasting inhibition in cluster 3 compared to cluster 1, which is 99 percent wS1.

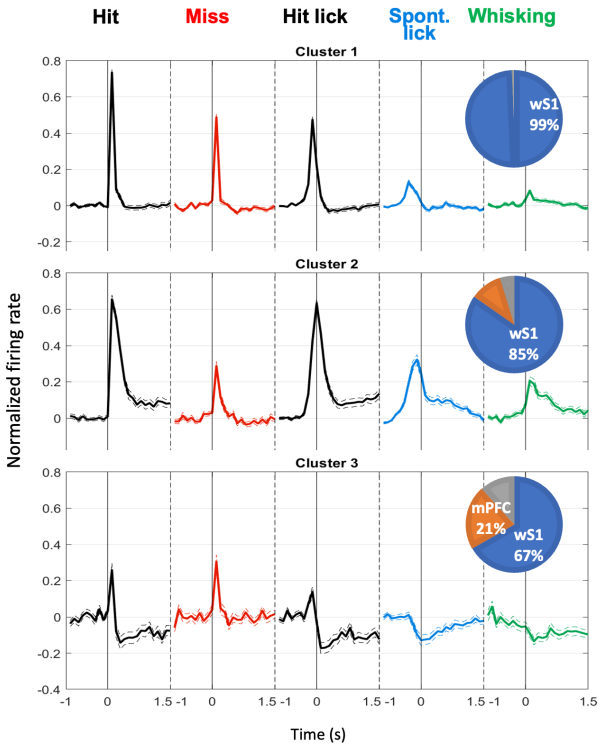

Figure 11: Clusters 1-3. Most representative clusters of wS1.

3.1.2 How motor information is represented by neuronal activity?

In figure 12, grand average PSTH of most representative clusters of tjM1 is shown. As demonstrated in the figure below, jaw opening-related clusters which contain mainly motor related neurons are widespread across the areas; however, cluster 5 is quite specific to tjM1 and there is not any activity in miss trials.

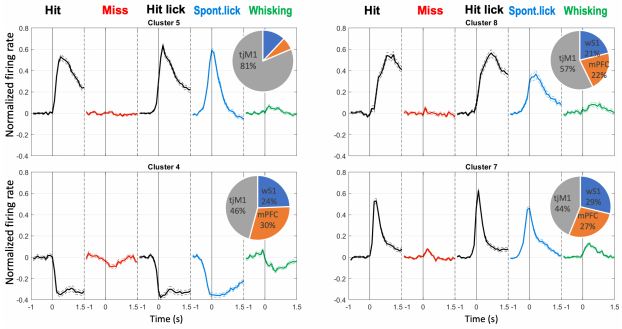

Figure 12: Clusters 4, 5, 7, 8. Most representative clusters of tjM1.

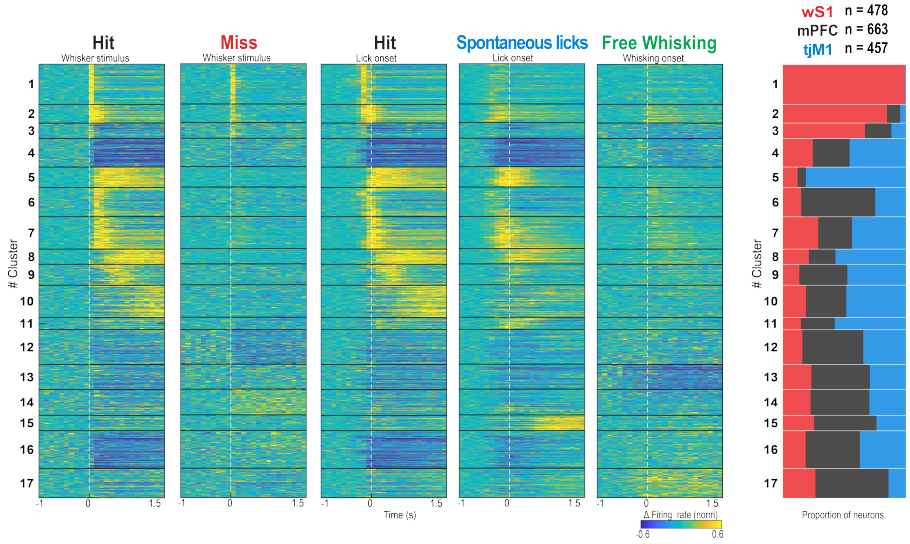

Figure 7: PSTH of all neurons clustered and weighted proportion of neurons within each cluster belonging to different brain regions.

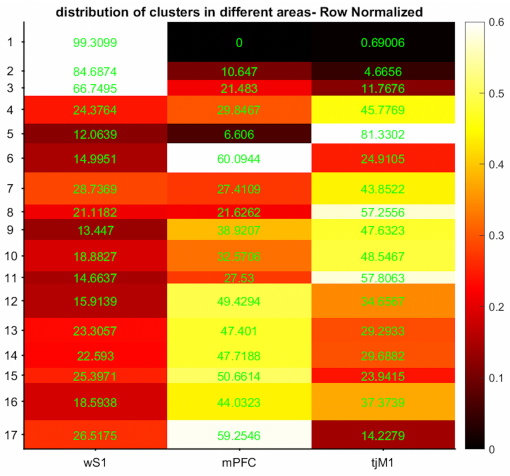

Figure 9: Composition of clusters. Weighted proportion of neurons within each cluster belonging to different brain regions

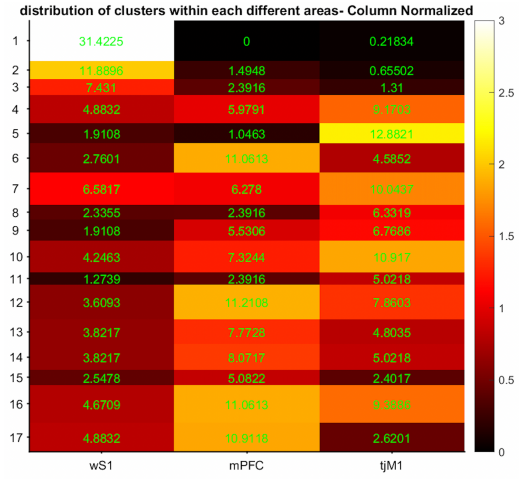

Figure 10: Composition of areas. Weighted proportion of neurons within each area belonging to different clusters

3.1.3 How choice information is represented by neuronal activity?

For the Identification of choice or decision neurons, they should exhibit activity in hit trials but not in miss and spontaneous licking trials as the decision is defined to lick the spout in presence of a whisker stimulus. Despite having minor activity in miss and spontaneous lick trials, cluster 6 is the closest to the definition of choice neurons between all clusters and choice neurons are sub-group of this cluster (Figure 13). Choice neurons are distributed across areas but more in mPFC.

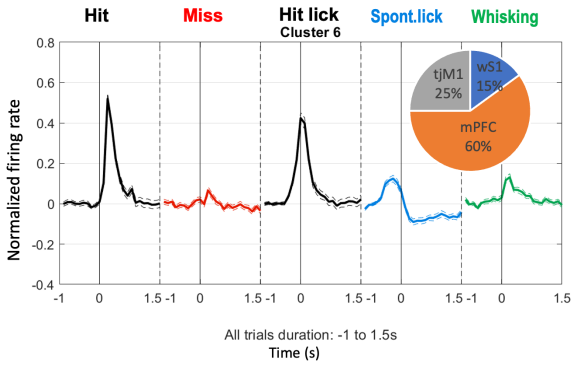

Figure 13: Cluster 6. The most representative cluster of mPFC.

3.1.4 What else is represented in mPFC?

Two of the clusters, 15 and 14, display an intriguing pattern of activity that may indicate a role for the areas, most notably the mPFC, in the generation of teaching signals for learning by error (Figure 14). Cluster 15 demonstrates that there is a maximal activity in spontaneous licks that do not match motor activity since it is absent in hit trials and may signal the absence of the reward despite licking (reward expectation). Cluster 14 reveals that there is a maximal activity when the reward is missed and may signal the mice not doing the task correctly.

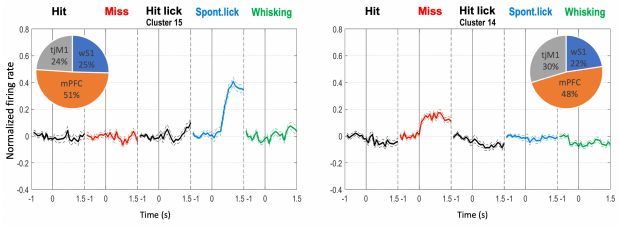

Figure 14: Clusters 14 and 15. Error (teaching) signal in mPFC.

3.2. Interareal connectivity analysis

To examine how the coordination between sensory and motor cortices changed throughout the course of learning, interareal interactions were assessed among wS1->wM1 and wS2->wM2 in the subset of sessions in which simultaneous paired recordings from these regions were collected (Figure 15 and Figure 16). Averaged over individual pairs of neurons, trial-by-trial correlation between evoked activity of wS2-RS units with wM2-RS units increased across learning while it decreased between wS2-RS units and wM2-FS units. These apparent changes in correlations may be influenced by variations in firing rates caused by learning. Despite the fact that the activity of wM1 FS units increased with learning, the correlation between wS1-RS units and wM1-FS units did not alter considerably, nor did the connection between wS1-RS units and wM1-RS units. As a further control, interareal pairwise correlations utilizing the spike time tiling coefficient (STTC) approach were assessed [2], which is believed to be insensitive to firing rate (Figure 17B). Using STTC analysis, the only significant increase in correlation across learning was found between wS2-RS and wM2-RS units. Trial-by-trial correlation of the population response showed similar patterns of change across learning in both area pairs as those observed in pair-wise correlation changes (Figure 17A). To further analyze changes in functional connectivity, the amount of directional connections (putative direct monosynaptic connections) were determined based on short-latency sharp peaks in the cross-correlograms between pairs of neurons from the whisker sensory and whisker motor cortices (Figure 16 and 17C). The number of linkages between wS2-RS units and wM2-RS units increased significantly as learning progressed. These findings show that learning increases the ratio of excitation to inhibition in the sensory-evoked response in wM2, but decreases it in wM1 in favor of inhibition. Increased functional connectivity between wS2 and wM2 may result in increased activity of excitatory neurons in wM2 in answer to learning.

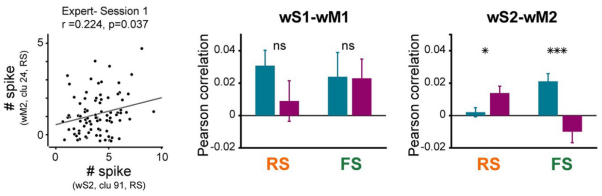

Figure 15: Pair-wise correlation between sensory and motor cortices in Novice and Expert mice. Left: A scatter plot illustrating the trial-by-trial correlation between the whisker-evoked response of a sample pair of neurons in wS2 and wM2. Each circle indicates the neural pair's response in a 1 trial. The circles were slightly jittered for viewing purposes. Gray line: least-squares regression. Middle: Average pair-wise Pearson correlation of wS1-RS units with wM1-RS and wS1-RS units with wM1-FS units separately. Right: Average pair-wise Pearson correlation between wS2-RS units and wM2-RS units and wS2-RS units and wM2-FS units. Error bars: SEM. The Wilcoxon rank-sum test was used to compare Novice and Expert statistically (ns: p > = 0.05; *: p 0.05; ***: p 0.001).

4. Conclusions

Clusters with wS1 majorities are characterized by a transient, rapid, and sharp activation in response to the whisker stimulation (hit and miss trails), and the majority of neurons of these clusters (1, 2, and 3) are identified as sensory

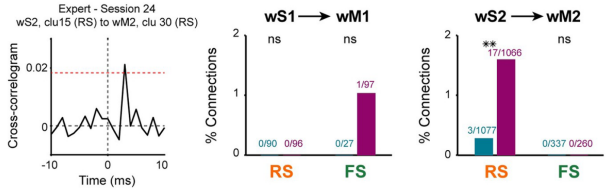

Figure 16: Left: Example of a cross-correlogram between two neurons from wS2 and wM2 simultaneously recorded. A directional connection between wS2 and wM2 has been detected due to a threshold crossing between 0 and 10 milliseconds. Middle: Percentage of discovered connections from wS1-RS to wM1-RS and wM1-FS. Right: Percentage of discovered directional connections from wS2-RS to wM2-RS and wM2-FS units. The numbers on each bar show the total number of discovered connections and recorded pairs.

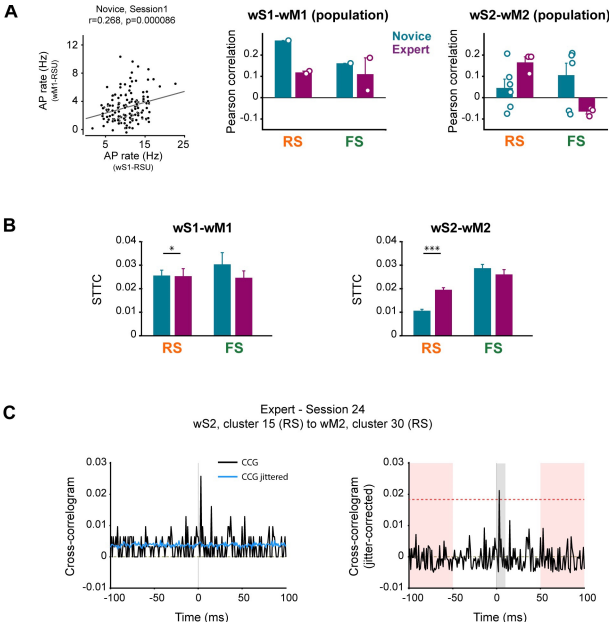

Figure 17: (A) Interareal correlation of population response in Novice and Expert mice. (Left) Scatter plot of the average trial-by-trial population response between wS1-RS units and wM1-RS units for a Novice session. Gray line: Pearson correlation of trial-by-trial average population response of wS1-RS and wM1-RS and wS1-RS and wM1-FS units. (Right) Pearson correlation of trial-by-trial population average response of wS2-RS vs wM2-RS and wS2-RS versus wM2-FS units. Circles represent separate sessions. Error bars: SEM. (B) Correlation between the sensory and motor cortices of novice and expert mice utilizing the STTC technique. Left: Average pair-wise STTC correlation of wS1-RS units with wM1-RS and wS1-RS units with wM1-FS units. Right: Average pair-wise Pearson correlation between wS2-RS units and wM2-RS and wS2-RS units and wM2-FS units. Error bars: SEM. (C) Example cross-correlogram (CCG) from a pair of neurons simultaneously recorded in wS2 and wM2 of an Expert mouse with a significant connection; similar example pair as in Figure 16, but with CCG from -100 to 100 ms time lags. Jitter correction approach (left) and significant functional connections detection (right). Significant connections were detected if any threshold crossing happened within 0- to 10-ms time lags (gray bar) of the jitter-corrected CCG. Threshold (red dotted line) was defined as 6-fold standard deviation of the jitter-corrected CCG flanks (red bars).

neurons. Clusters composed primarily of tjM1 neurons (clusters 4, 5, 7, and 8) participate in movement-related functions (hit and spontaneous licks trials) and are predominantly composed of motor related neurons. On the other hand, it is believed that mPFC plays a role in sensory input to motor output cooperating in the integration. Clusters composed primarily of mPFC neurons (clusters 6, 14, and 15) exhibit complicated behaviors that may indicate the mPFC's probable participation in learning and teaching, resulting in improved decision-making. Particularly, cluster 6 could indicate choice neurons with strong excitation in hit trials and minor activity in miss and spontaneous lick trails. Moreover, clusters 14 and 15, could show an error signal pointing to not receiving the reward.

On a different study in connectivity analysis, It has been found out that RS units in wM1 decreased their sensory-evoked response over the course of learning, but RS units in wM2 increased their response [4]. Trial-by-trial correlations (Figure 15) and spike-triggered connectivity analyses (Figure 16) both indicated enhanced coupling between wS2-RS units and wM2-RS units, which could, at least in part, result from potentiation of monosynaptic inputs from wS2-RS units to wM2-RS units, although other more complex mechanisms could also play a role. In contrast, FS units in wM1 increased their response over the course of learning, while

FS units in wM2 decreased their evoked neuronal activity. Findings indicate that the balance between excitation and inhibition changes differentially with learning in wM1 and wM2, with improved sensory-evoked inhibition relative to excitation in wM1 and enhanced sensory-evoked excitation relative to inhibition in wM2. Changes in inhibitory neural activity may play a significant role in task learning. Throughout learning, increased recruitment of rapid inhibition in wM1 may reduce the response of excitatory neurons in wM1. It is hypothesized that inhibiting wM1 activity could improve whisker detection performance by minimizing whisker movements, which could otherwise lead to sensory reafference signals. On the other hand, the decreased firing of inhibitory neurons in wM2 during learning may permit the excitatory neurons to react more strongly.

References

[1] Emmanuel Abbe. Community detection and stochastic block models: recent developments. *The Journal of Machine Learning Research*, 18(1):6446–6531, 2017.

[2] Catherine S Cutts and Stephen J Eglen. Detecting pairwise correlations in spike trains: an objective comparison of methods and application to the study of retinal waves. *Journal of Neuroscience*, 34(43):14288–14303, 2014.

[3] Ben Engelhard, Joel Finkelstein, Julia Cox, Weston Fleming, Hee Jae Jang, Sharon Ornelas, Sue Ann Koay, Stephan Y Thiberge, Nathaniel D Daw, David W Tank, et al. Specialized coding of sensory, motor and cognitive variables in vta dopamine neurons. *Nature*, 570(7762):509–513, 2019.

[4] Vahid Esmaeili, Keita Tamura, Samuel P Muscinelli, Alireza Modirshanechi, Marta Boscaglia, Ashley B Lee, Anastasiia Oryshchuk, Georgios Foustoukos, Yanqi Liu, Sylvain Crochet, et al. Rapid suppression and sustained activation of distinct cortical regions for a delayed sensory-triggered motor response. *Neuron*, 109(13):2183–2201, 2021.

[5] Alexis Ortiz-Rosario, Hojjat Adeli, and John A Buford. Music-expected maximization gaussian mixture methodology for clustering and detection of task-related neuronal firing rates. *Behavioural brain research*, 317:226–236, 2017.

[6] Markus Siegel, Timothy J Buschman, and Earl K Miller. Cortical information flow during flexible sensorimotor decisions. *Science*, 348(6241):1352–1355, 2015.

[7] Joshua H Siegle, Xiaoxuan Jia, Séverine Durand, Sam Gale, Corbett Bennett, Nile Graddis, Greggory Heller, Tamina K Ramirez, Hannah Choi, Jennifer A Luviano, et al. Survey of spiking in the mouse visual system reveals functional hierarchy. *Nature*, 592(7852):86–92, 2021.

Acknowledgements

The research reported in this dissertation was undertaken between September 2021 and April 2022 at the LSENS group - Brain Mind Institute - EPFL. I'd like to thank Prof. Pedrocchi and Prof. Petersen for allowing me to embark on this journey. Thank you for having faith in me and for your support. Dear Sylvain, you have been an amazing coach. I would want to thank you for allowing me to pursue my hobbies and always ensuring that I was on the right route. This thesis would not have been possible without your contribution, incisive feedback, and supervision, Vahid, Anastasiia, and Alireza. Thank you guys!!